Search for the production of dark matter in association with top-quarks in the single-lepton final state in proton-proton collisions at $\sqrt{s} = 8\,TeV$

João A. Gonçalves

Paper may be found here

IST
LIP
CMS

05/06/2017

Outline

TÉCNICO LISBOA

Introduction

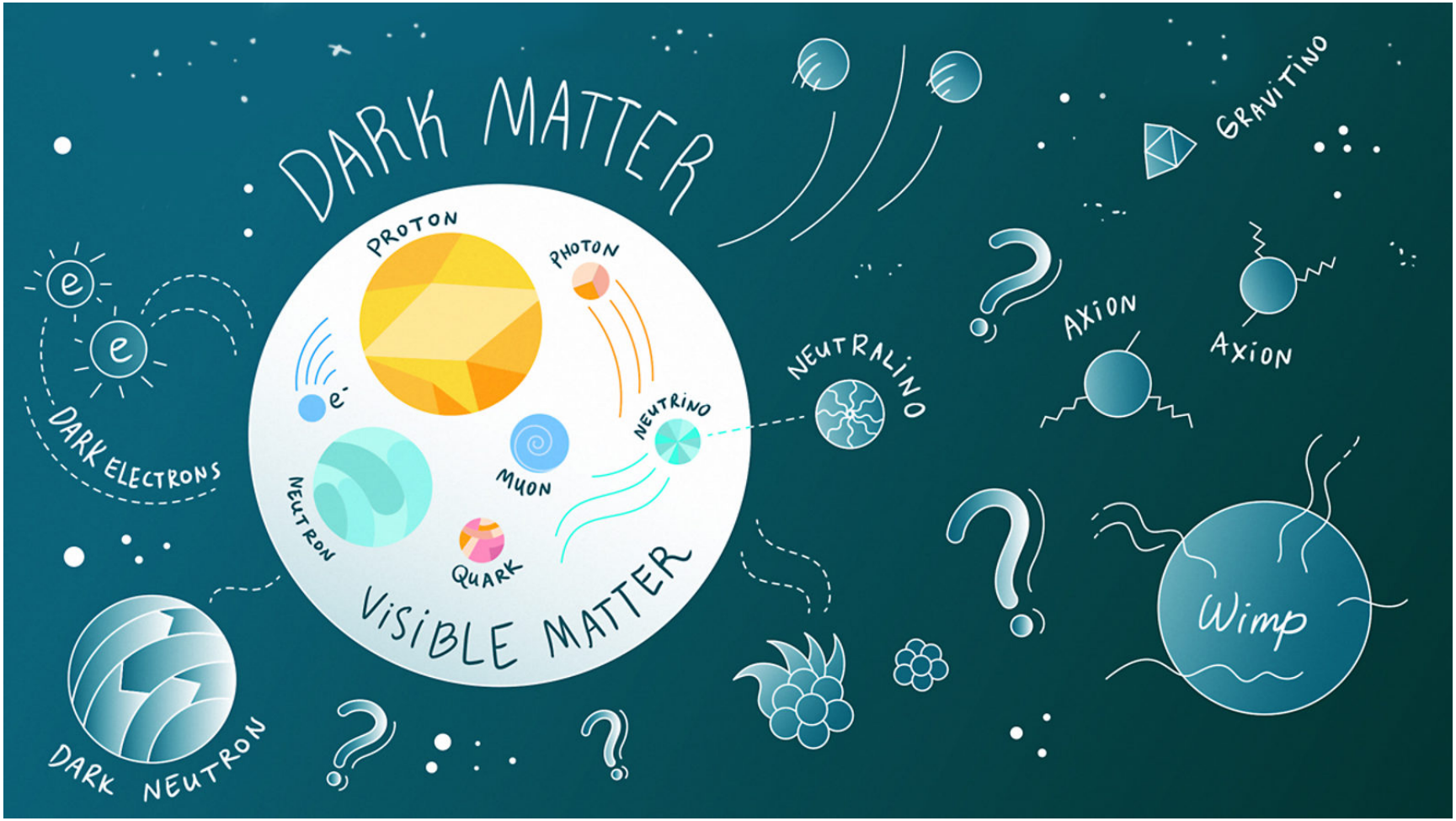

Introduction

$$L_{\text{int}} = \sum_{q} \sum_{i} C_{q\,i} \, (\bar{q} \Gamma_i^q q) \, (\bar{\chi} \Gamma_i^{\chi} \chi)$$

Introduction

$$L_{\text{int}} = \sum_{q} \sum_{i} C_{q\,i} \, (\bar{q} \Gamma_i^q \mathrm{q}) \, (\bar{\chi} \Gamma_i^{\chi} \chi)$$

Γ represents the type of interaction.

Introduction

$$L_{\text{int}} = \sum_{q} \sum_{i} c_{q\,i} \, (\bar{q} \Gamma_i^q q) \, (\bar{\chi} \Gamma_i^\chi \chi)$$

In this scenario we can have the production of DM particles associated with :

- a monojet. [1] [3] [4] [5] [6] [7] [8]
- a monophoton. [4]
- a W/Z boson. [9]

Introduction

$$L_{\text{int}} = \sum_{q} \sum_{i} C_{q\,i} \left(\bar{q} \Gamma_i^q \mathrm{q}\right) \left(\bar{\chi} \Gamma_i^{\chi} \chi\right)$$

$$L_{\text{int}} = \frac{m_{\mathrm{q}}}{M_*^3} \bar{q} q \bar{\chi} \chi$$

Introduction

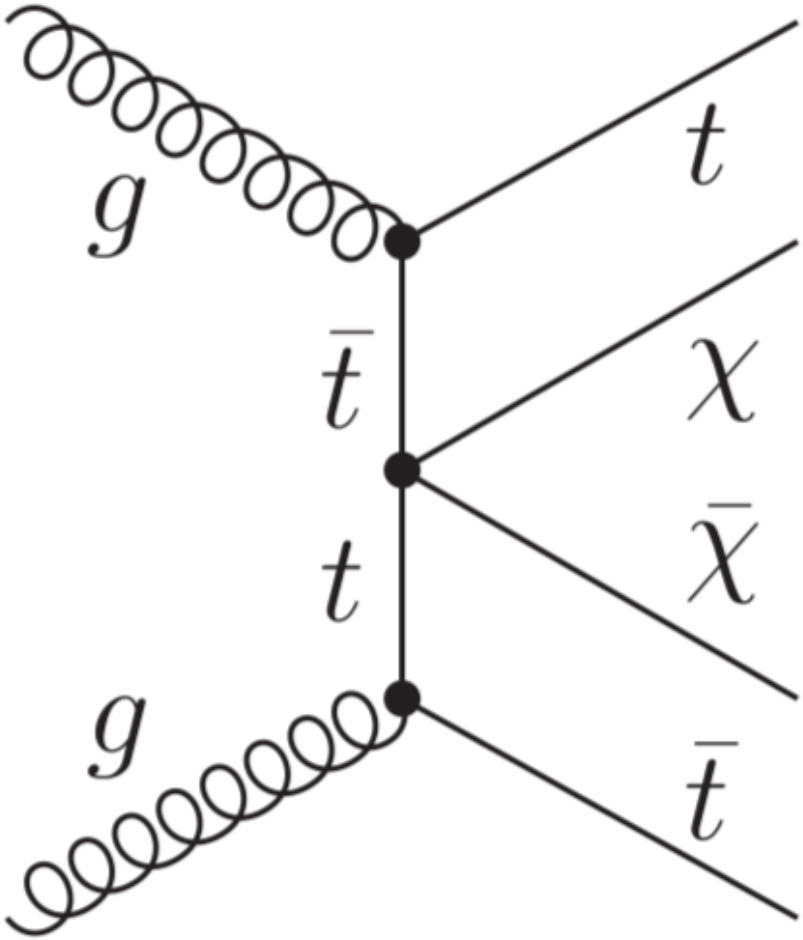

The CMS detector

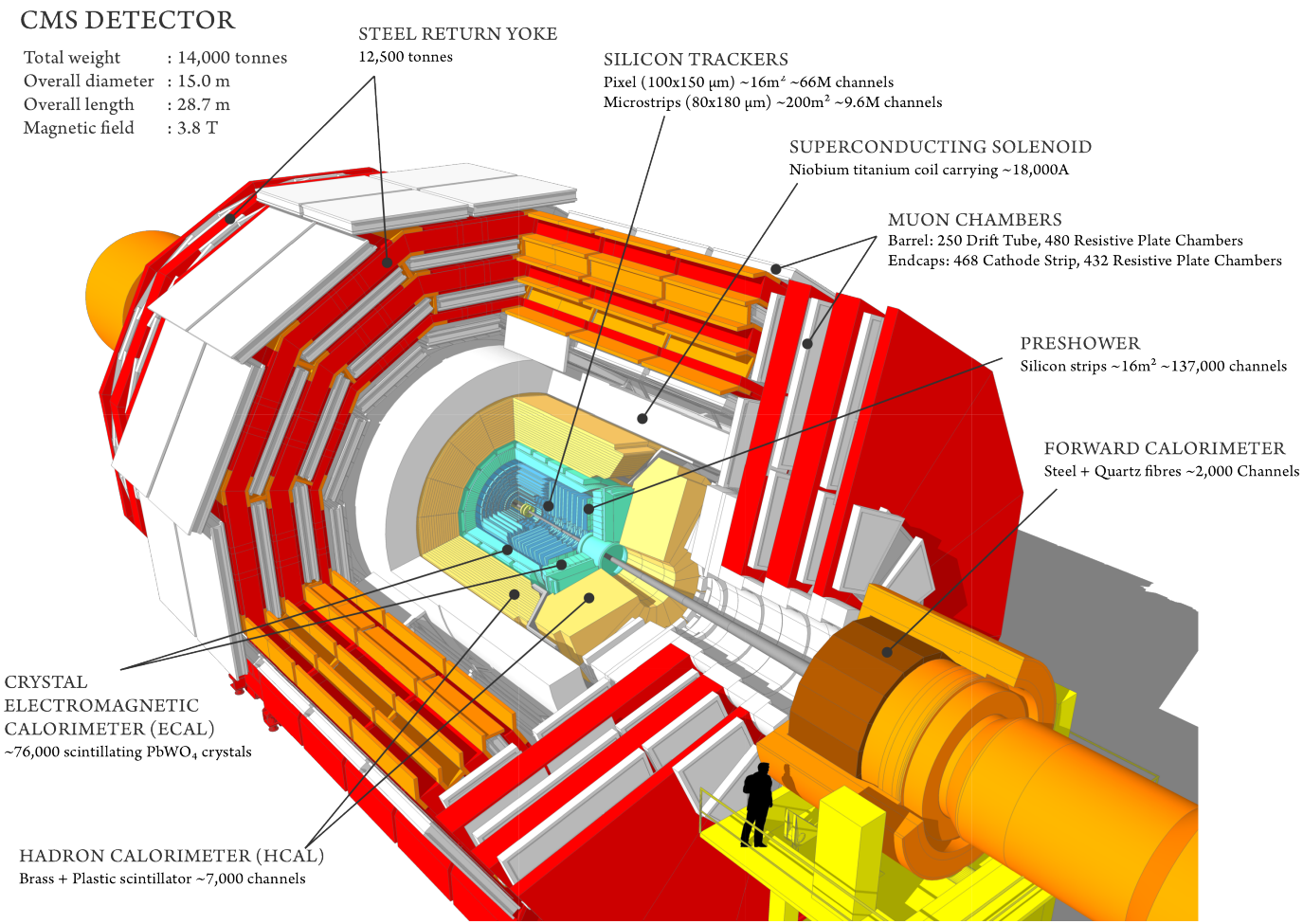

More on the detector and kinematic coordinate system at [13]

Data and simulated samples

Data

- Data recorded on the CMS experiment at the LHC.

Data and simulated samples

Data

- Data recorded on the CMS experiment at the LHC.
- $\sqrt{s} = 8\,TeV$.

Data and simulated samples

Data

- Data recorded on the CMS experiment at the LHC.
- $\sqrt{s} = 8 TeV$.
- $\int L dt = 19.7 fb^{-1}$.

Data and simulated samples

Data

- Data recorded on the CMS experiment at the LHC.
- $\sqrt{s} = 8 TeV$.
- $\int Ldt = 19.7 fb^{-1}$.
- Single-electron trigger $p_T > 27 Gev$.

Data and simulated samples

Data

- Data recorded on the CMS experiment at the LHC.
- $\sqrt{s} = 8 TeV$.
- $\int Ldt = 19.7 fb^{-1}$.
- Single-electron trigger $p_T > 27 Gev$.
- Single-muon trigger $p_T > 24 GeV$.

Data and simulated samples

Data

- Data recorded on the CMS experiment at the LHC.
- $\sqrt{s} = 8 TeV$.
- $\int Ldt = 19.7 fb^{-1}$.
- Single-electron trigger $p_T > 27 Gev$.
- Single-muon trigger $p_T > 24 GeV$.
- Efficiencies of these triggers in data and simulation are compared and measured using a tag-probe method : [14].

Data and simulated samples

Simulation

- Dark matter signals are generated with MADGRAPH v5.1.5.11 : [15].

Data and simulated samples

Simulation

- Dark matter signals are generated with MADGRAPH v5.1.5.11 : [15].
- Leading order matrix element generator using the CTEQ6L1 PDF's : [16].

Data and simulated samples

Simulation

- Dark matter signals are generated with MADGRAPH v5.1.5.11 : [15].
- Leading order matrix element generator using the CTEQ6L1 PDF's : [16].
- The dominat backgrounds are $t\bar{t}$+jets, $t\bar{t}$ + γ/W/Z, W+jets, single top, diboson and Drell-Yan events.

Data and simulated samples

Simulation

- Dark matter signals are generated with MADGRAPH v5.1.5.11 : [15].
- Leading order matrix element generator using the CTEQ6L1 PDF's : [16].
- All backgrounds except single top and WW events are generated with MADGRAPH using CTEQ6L1 PDF.

Data and simulated samples

Simulation

- Dark matter signals are generated with MADGRAPH v5.1.5.11 : [15].
- Leading order matrix element generator using the CTEQ6L1 PDF's : [16].
- All backgrounds except single top and WW events are generated with MADGRAPH using CTEQ6L1 PDF.
- Single top processes are generated at NLO with POWHEG v1.0 with the CTEQ6M PDF [16].

Data and simulated samples

Simulation

- Dark matter signals are generated with MADGRAPH v5.1.5.11 : [15].
- Leading order matrix element generator using the CTEQ6L1 PDF's : [16].
- All backgrounds except single top and WW events are generated with MADGRAPH using CTEQ6L1 PDF.
- Single top processes are generated at NLO with POWHEG v1.0 with the CTEQ6M PDF [16].
- The WW background is generated with PYTHIA v6.424 [18].

Data and simulated samples

Simulation

- All events generated with MADGRAPH are matched to PYTHIA, and all events are passes through the CMS detector simulation GEANT4 v9.4 [19].

Data and simulated samples

Simulation

- All events generated with MADGRAPH are matched to PYTHIA, and all events are passes through the CMS detector simulation GEANT4 v9.4 [19].

- Cross sections of $t\bar{t} + jets$ [20] and W/Z + jets [21] are calculated at NNLO.

Data and simulated samples

Simulation

- All events generated with MADGRAPH are matched to PYTHIA, and all events are passes through the CMS detector simulation GEANT4 v9.4 [19].
- Cross sections of $t\bar{t} + jets$ [20] and W/Z + jets [21] are calculated at NNLO.
- Other backgrounds are calculated at NLO (single top [22], $t\bar{t}$ + Z [23], $t\bar{t}$ +W [24], $t\bar{t}$ + γ [25] and diboson [26]).

TÉCNICO LISBOA LIP

Object reconstruction

- A particle-flow (PF) based event reconstruction, taking into account information from all subdetectros, is used. [27] [28]

Object reconstruction

- A particle-flow (PF) based event reconstruction, taking into account information from all subdetectros, is used. [27] [28]
- Primary vertices are reconstructed using a deterministic annealing filter algorithm, and are defined as the vertex with the largest sum of squares of the p_T of the tracks associated to it.

.

Object reconstruction

Electrons

- Electrons are reconstructed from energy cluster deposits in ECAL matched with tracks [30].

Object reconstruction

Electrons

- Electrons are reconstructed from energy cluster deposits in ECAL matched with tracks [30].
- Electrons are required not to be in $1.44 < |\eta| < 1.57$, since this is the transition region from barrel to end-cap and the reconstruction there is not optimal.

Object reconstruction

Electrons

- Electrons are reconstructed from energy cluster deposits in ECAL matched with tracks [30].
- Electrons are required not to be in $1.44 < |\eta| < 1.57$, since this is the transition region from barrel to end-cap and the reconstruction there is not optimal.
- After all the requirements electrons are accepted if they have a p_T > 30 GeV and $|\eta|$ < 2.5.

Object reconstruction

Muons

- Muons are reconstructed by combining tracks and muon system resulting in "global-muon tracks". [32]

Object reconstruction

Muons

- Muons are reconstructed by combining tracks and muon system resulting in "global-muon tracks". [32]

- Muons from cosmic rays and other unwanted sources are supressed by applying quality requirements on the global-muon fit amoung other relevant variables.

Object reconstruction

Muons

- Muons are reconstructed by combining tracks and muon system resulting in "global-muon tracks". [32]
- Muons from cosmic rays and other unwanted sources are supressed by applying quality requirements on the global-muon fit amoung other relevant variables.
- After all the requirements muons are accepted if they have a $p_T >$ 30 GeV, $|\eta| < 2.1$ and $R^{\mu}_{Iso} < 0.12$.

Object reconstruction

Muons

- Muons are reconstructed by combining tracks and muon system resulting in "global-muon tracks". [32]
- Muons from cosmic rays and other unwanted sources are supressed by applying quality requirements on the global-muon fit amoung other relevant variables.
- After all the requirements muons are accepted if they have a $p_T >$ 30 GeV, $|\eta| < 2.1$ and $R^{\mu}_{Iso} < 0.12$.
- Electrons and muon efficiencies are measured via the tag-and-probe technique using inclusive samples of leptonically decaying Z bosons, from data and simulation.

Object reconstruction

Jets and CSV

- Jets are reconstructed from PF candidates, that are clustered with the anti-k_T algorithm [33] with R=0.5 using FASTJET. [34].

Object reconstruction

Jets and CSV

- Jets are reconstructed from PF candidates, that are clustered with the anti-k_T algorithm [33] with R=0.5 using FASTJET. [34].
- Jet candidates are required to have $p_T > 30$ GeV, $|\eta| < 4$ and satisfy a loose set of quality criteria available at the reference.

.

Object reconstruction

Jets and CSV

- Jets are reconstructed from PF candidates, that are clustered with the anti-k_T algorithm [33] with R=0.5 using FASTJET. [34].
- Jet candidates are required to have $p_T > 30$ GeV, $|\eta| < 4$ and satisfy a loose set of quality criteria available at the reference.
  .
- Combined secondary vertex (CSV) b-tagging algorithm is used to identify b-jets.

Object reconstruction

Jets and CSV

- Jets are reconstructed from PF candidates, that are clustered with the anti-k_T algorithm [33] with R=0.5 using FASTJET. [34].
- Jet candidates are required to have $p_T > 30$ GeV, $|\eta| < 4$ and satisfy a loose set of quality criteria available at the reference.
  .
- Combined secondary vertex (CSV) b-tagging algorithm is used to identify b-jets.
- It combines the relevant information in a likelihood discriminant providing a continuous output from 0 to 1.

Object reconstruction

Jets and CSV

- Jets are reconstructed from PF candidates, that are clustered with the anti-k_T algorithm [33] with R=0.5 using FASTJET. [34].
- Jet candidates are required to have $p_T > 30$ GeV, $|\eta| < 4$ and satisfy a loose set of quality criteria available at the reference.
  .
- Combined secondary vertex (CSV) b-tagging algorithm is used to identify b-jets.
- It combines the relevant information in a likelihood discriminant providing a continuous output from 0 to 1.
- A jet is b-tagged if the discriminant output is greater than .679 and $|\eta| < 2.4$.

Event selection

Preselection

- $N_{Jets} \geq 3$. (+10% sensitivity than ≥ 4)

Event selection

Preselection

- $N_{Jets} \geq 3$. (+10% sensitivity than ≥ 4)
- $N_{b-jets} \geq 1$.

Event selection

Preselection

- $N_{Jets} \geq 3$. (+10% sensitivity than ≥ 4)
- $N_{b-jets} \geq 1$.
- $N_{Iso} = 1$.

Event selection

Preselection

- $N_{Jets} \geq 3.$ (+10% sensitivity than ≥ 4)
- $N_{b-jets} \geq 1.$
- $N_{Iso} = 1.$
- $E_T^{miss} > 160$ GeV.

Event selection

Preselection

- $N_{Jets} \geq 3$. (+10% sensitivity than ≥ 4)
- $N_{b-jets} \geq 1$.
- $N_{Iso} = 1$.
- $E_T^{miss} > 160$ GeV.
- After this preselection the dominant backgrounds are from $t\bar{t}$ and W + jets production.

Event selection

Preselection

- $N_{Jets} \geq 3$. (+10% sensitivity than ≥ 4)
- $N_{b-jets} \geq 1$.
- $N_{Iso} = 1$.
- $E_T^{miss} > 160$ GeV.
- After this preselection the dominant backgrounds are from $t\bar{t}$ and W + jets production.
- Other backgrounds include single top, Drell-Yan and diboson. QCD multijet background is negligible within these requirements.

Event selection

Selection

- $E_T^{miss} > 320 GeV$.

Event selection

Selection

- $E_T^{miss} > 320 GeV$.
- The remaining W + jets and most $t\bar{t}$ backgrounds contain a single leptonically decaying W boson.

Event selection

Selection

- $E_T^{miss} > 320 GeV$.
- The remaining W + jets and most $t\bar{t}$ backgrounds contain a single leptonically decaying W boson.
- Defining the transverse mass as :
  $M_T = \sqrt{2 E_T^{miss} p_T^l (1 - cos(\Delta\phi)}$.

Event selection

Selection

- $E_T^{miss} > 320 GeV$.
- The remaining W + jets and most $t\bar{t}$ backgrounds contain a single leptonically decaying W boson.
- Defining the transverse mass as :
  $M_T = \sqrt{2 E_T^{miss} p_T^l (1 - cos(\Delta\phi)}$.
- M_T > 160 GeV cut is applied.

Event selection

Selection

- $E_T^{miss} > 320 GeV$.
- The remaining W + jets and most $t\bar{t}$ backgrounds contain a single leptonically decaying W boson.
- Defining the transverse mass as :
  $M_T = \sqrt{2 E_T^{miss} p_T^l (1 - cos(\Delta\phi)}$.
- M_T > 160 GeV cut is applied.
- The dominat background becomes dileptonic $t\bar{t}$ events, with one lepton unobserved.

Event selection

Selection

- The variable M_{T2}^{W} is used to further reduce this background.

$$M_{\mathrm{T2}}^{\mathrm{W}} = \min\left(m_{\mathrm{y}} \text{ consistent with: } \left\{ \begin{array}{l} \vec{p}_1^{\,\mathrm{T}} + \vec{p}_2^{\,\mathrm{T}} = \vec{p}_{\mathrm{T}}^{\,\mathrm{miss}}, p_1^2 = 0, (p_1 + p_\ell)^2 = p_2^2 = M_{\mathrm{W}}^2, \\ (p_1 + p_\ell + p_{\mathrm{b1}})^2 = (p_2 + p_{\mathrm{b2}})^2 = m_{\mathrm{y}}^2 \end{array} \right\}\right)$$

Event selection

Selection

- The variable M_{T2}^{W} is used to further reduce this background.

$$M_{\mathrm{T2}}^{\mathrm{W}} = \min\left(m_{\mathrm{y}} \text{ consistent with: } \left\{ \begin{array}{l} \vec{p}_1^{\,\mathrm{T}} + \vec{p}_2^{\,\mathrm{T}} = \vec{p}_{\mathrm{T}}^{\,\mathrm{miss}}, p_1^2 = 0, (p_1 + p_\ell)^2 = p_2^2 = M_{\mathrm{W}}^2, \\ (p_1 + p_\ell + p_{\mathrm{b1}})^2 = (p_2 + p_{\mathrm{b2}})^2 = m_{\mathrm{y}}^2 \end{array} \right\}\right)$$

- The selected events have $M_{T2}^{W} > 200$ GeV.

Event selection

Selection

- The variable M_{T2}^{W} is used to further reduce this background.

$$M_{\mathrm{T2}}^{\mathrm{W}} = \min\left(m_{\mathrm{y}} \text{ consistent with: } \left\{ \begin{array}{l} \vec{p}_1^{\,\mathrm{T}} + \vec{p}_2^{\,\mathrm{T}} = \vec{p}_{\mathrm{T}}^{\,\mathrm{miss}}, p_1^2 = 0, (p_1 + p_\ell)^2 = p_2^2 = M_{\mathrm{W}}^2, \\ (p_1 + p_\ell + p_{\mathrm{b1}})^2 = (p_2 + p_{\mathrm{b2}})^2 = m_{\mathrm{y}}^2 \end{array} \right\}\right)$$

- The selected events have $M_{T2}^{W} > 200$ GeV.

- Finnaly the jets and the missing p_T tend to be more separated in ϕ in signal events than in $t\bar{t}$ backgrounds.

Event selection

Selection

- The variable M_{T2}^{W} is used to further reduce this background.

$$M_{\mathrm{T2}}^{\mathrm{W}} = \min\left(m_{\mathrm{y}} \text{ consistent with: } \left\{ \begin{array}{l} \vec{p}_1^{\,\mathrm{T}} + \vec{p}_2^{\,\mathrm{T}} = \vec{p}_{\mathrm{T}}^{\,\mathrm{miss}}, p_1^2 = 0, (p_1 + p_\ell)^2 = p_2^2 = M_{\mathrm{W}}^2, \\ (p_1 + p_\ell + p_{\mathrm{b1}})^2 = (p_2 + p_{\mathrm{b2}})^2 = m_{\mathrm{y}}^2 \end{array} \right\}\right)$$

- The selected events have $M_{T2}^{W} > 200$ GeV.
- Finnaly the jets and the missing p_T tend to be more separated in ϕ in signal events than in $t\bar{t}$ backgrounds.
- So we aply the cut $\Delta\phi(j_{1,2}, \vec{p_T^{miss}}) > 1.2$.

Event selection

Selection

- The variable M_{T2}^{W} is used to further reduce this background.

$$M_{\mathrm{T2}}^{\mathrm{W}} = \min\left(m_{\mathrm{y}} \text{ consistent with: } \left\{ \begin{array}{l} \vec{p}_1^{\,\mathrm{T}} + \vec{p}_2^{\,\mathrm{T}} = \vec{p}_{\mathrm{T}}^{\,\mathrm{miss}}, p_1^2 = 0, (p_1 + p_\ell)^2 = p_2^2 = M_{\mathrm{W}}^2, \\ (p_1 + p_\ell + p_{\mathrm{b1}})^2 = (p_2 + p_{\mathrm{b2}})^2 = m_{\mathrm{y}}^2 \end{array} \right\}\right)$$

- The selected events have $M_{T2}^{W} > 200$ GeV.
- Finnaly the jets and the missing p_T tend to be more separated in ϕ in signal events than in $t\bar{t}$ backgrounds.
- So we aply the cut $\Delta\phi(j_{1,2}, \vec{p_T^{miss}}) > 1.2$.
- These selection cuts are optimized based on the expected significance for DM masses between 1 and 1000 GeV.

Event selection

Variable distributions

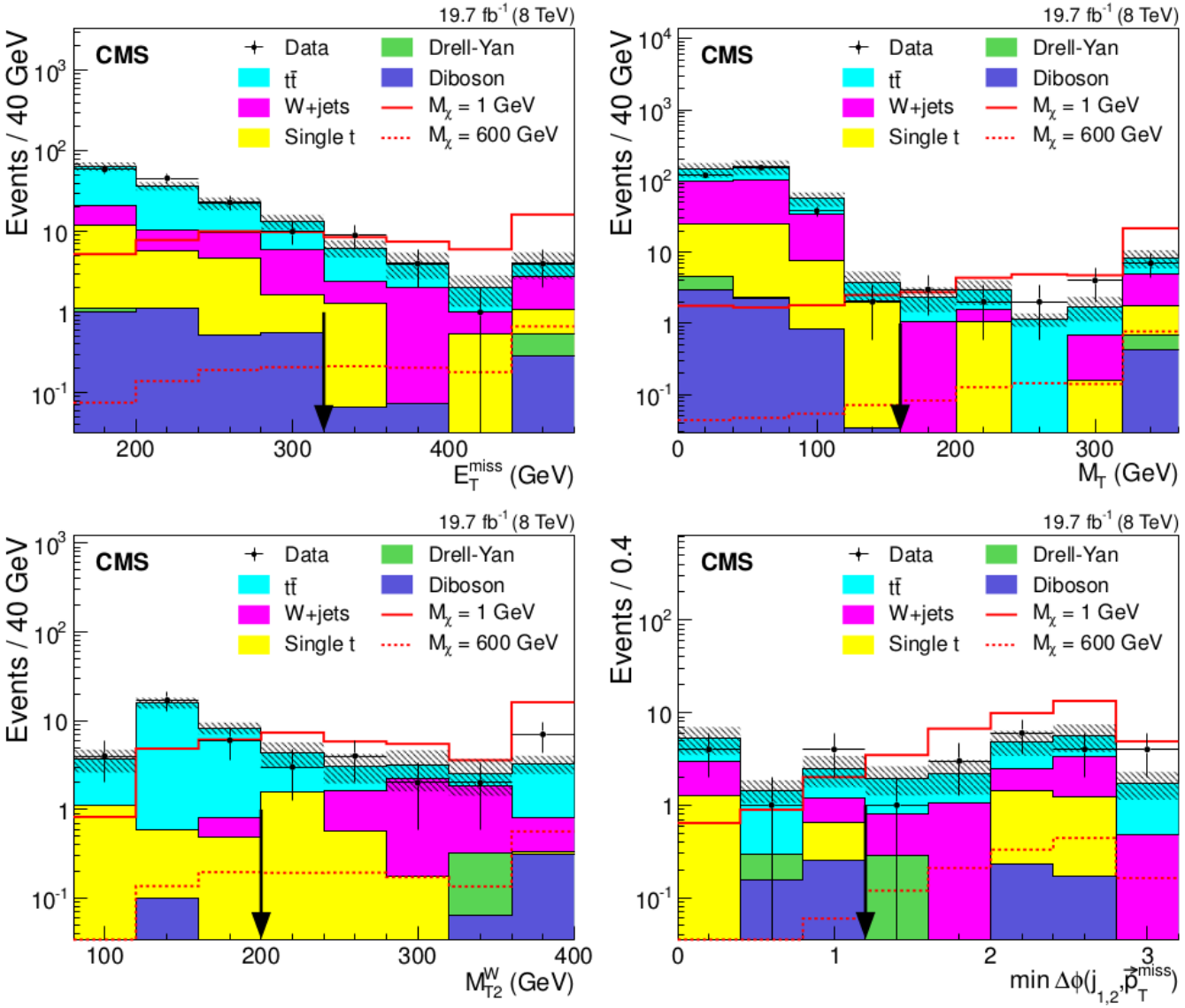

Background estimation

- Scale factor are applied to $t\bar{t}$ + jets and W + jets events dominat backgrounds to correct discrepancies between data and simulation.

Background estimation

- Scale factor are applied to $t\bar{t}$ + jets and W + jets events dominat backgrounds to correct discrepancies between data and simulation.
- Two control regions are defined to extract these SF's.

Background estimation

- Scale factor are applied to $t\bar{t}$ + jets and W + jets events dominat backgrounds to correct discrepancies between data and simulation.
- Two control regions are defined to extract these SF's.
- CR1 : preselection + M_T > 160 GeV. Which is dominated by $t\bar{t}$.

Background estimation

- Scale factor are applied to $t\bar{t}$ + jets and W + jets events dominat backgrounds to correct discrepancies between data and simulation.
- Two control regions are defined to extract these SF's.
- CR1 : preselection + $M_T > 160$ GeV. Which is dominated by $t\bar{t}$.
- CR2 : CR1 + $N_{b-jets} = 0$. Resulting in a W+jets enriched sample.

Background estimation

- Scale factor are applied to $t\bar{t}$ + jets and W + jets events dominat backgrounds to correct discrepancies between data and simulation.
- Two control regions are defined to extract these SF's.
- CR1 : preselection + $M_T > 160$ GeV. Which is dominated by $t\bar{t}$.
- CR2 : CR1 + $N_{b-jets} = 0$. Resulting in a W+jets enriched sample.
- SF's are obtained by matching data to the M_T distribution in the CR1, and the E_T^{miss} in the CR2.

Background estimation

- Scale factor are applied to $t\bar{t}$ + jets and W + jets events dominat backgrounds to correct discrepancies between data and simulation.
- Two control regions are defined to extract these SF's.
- CR1 : preselection + $M_T > 160$ GeV. Which is dominated by $t\bar{t}$.
- CR2 : CR1 + $N_{b-jets} = 0$. Resulting in a W+jets enriched sample.
- SF's are obtained by matching data to the M_T distribution in the CR1, and the E_T^{miss} in the CR2.
- The resulting SF's where $1.11 \pm 0.02(stat)$ and $1.26 \pm 0.06(stat)$ for $t\bar{t}$ and W respectively.

TÉCNICO LISBOA LIP

Background estimation

- Scale factor are applied to $t\bar{t}$ + jets and W + jets events dominat backgrounds to correct discrepancies between data and simulation.
- Two control regions are defined to extract these SF's.
- CR1 : preselection + $M_T > 160$ GeV. Which is dominated by $t\bar{t}$.
- CR2 : CR1 + $N_{b-jets} = 0$. Resulting in a W+jets enriched sample.
- SF's are obtained by matching data to the M_T distribution in the CR1, and the E_T^{miss} in the CR2.
- The resulting SF's where $1.11 \pm 0.02(stat)$ and $1.26 \pm 0.06(stat)$ for $t\bar{t}$ and W respectively.
- These scale factors are later propagated to the signal region to estimate the background.

TÉCNICO LISBOA LIP

Background Estimation

Distributions in control region 1

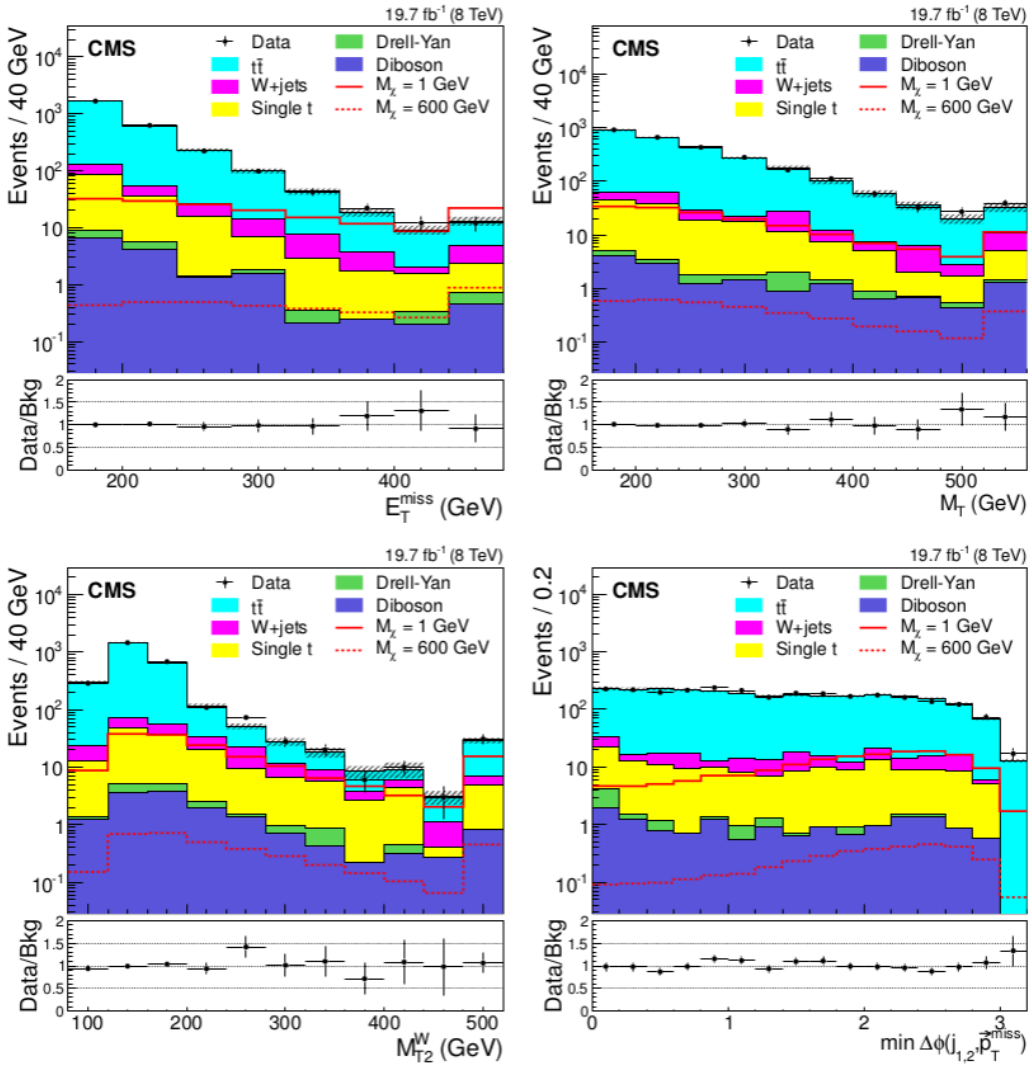

Background Estimation

Distributions in control region 2

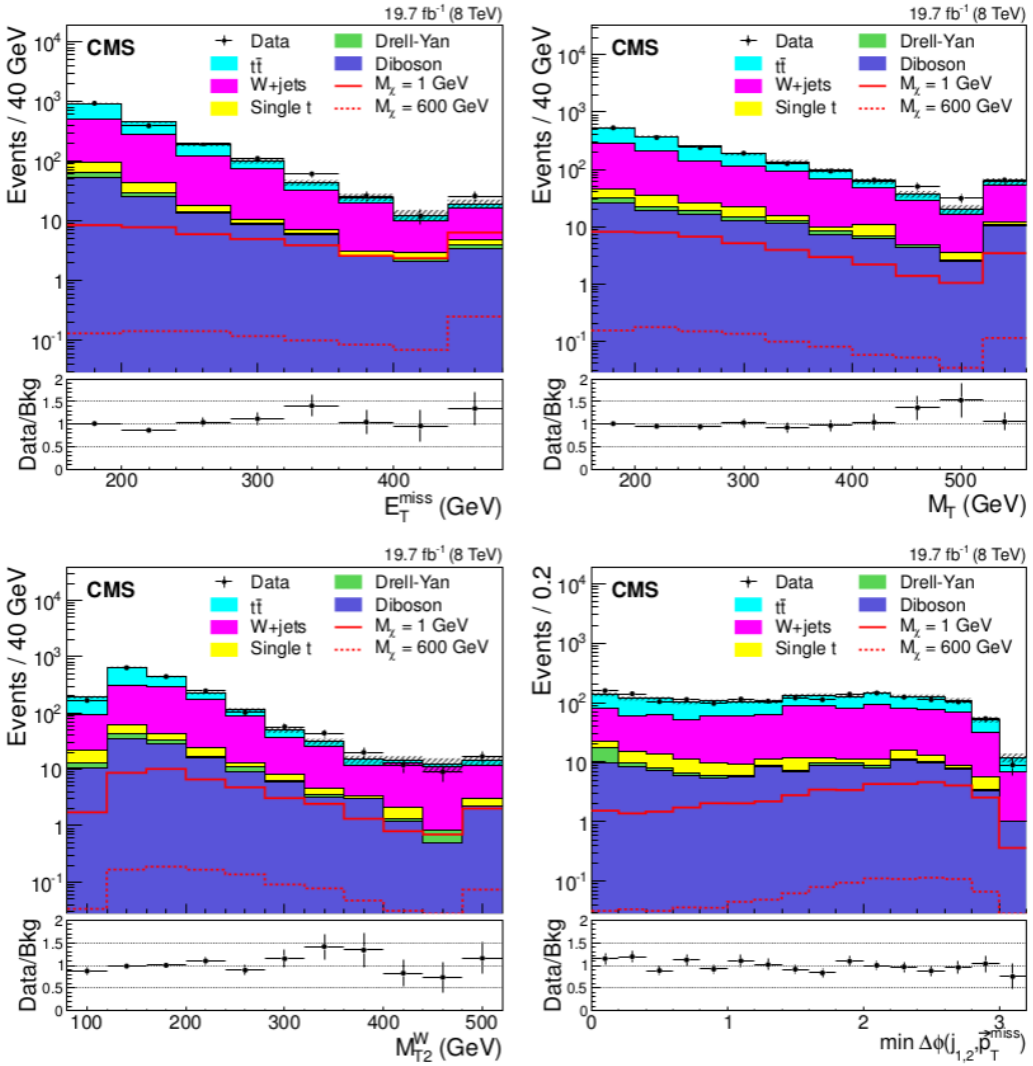

Systematic uncertainties

Source of systematic uncertainties	Relative uncertainty on total background (%)
50% normalization uncert. of other bkg in deriving SFs	10
SF_{W+jets} (CR tests)	13
$t\bar{t}$+jets top-quark p_T reweighting	3.9
Jet energy scale	4.0
Jet energy resolution	3.0
b-tagging correction factor (heavy flavour)	1.0
b-tagging correction factor (light flavour)	1.8
Pileup model	2.0
PDF	2.6

TÉCNICO LISBOA LIP

Results

Source	Yield ($\pm$stat $\pm$syst)
$t\bar{t}$	$8.2 \pm 0.6 \pm 1.9$
W	$5.2 \pm 1.8 \pm 2.1$
Single top	$2.3 \pm 1.1 \pm 1.1$
Diboson	$0.5 \pm 0.2 \pm 0.2$
Drell–Yan	$0.3 \pm 0.3 \pm 0.1$
Total Bkg	$16.4 \pm 2.2 \pm 2.9$
Data	18

For M_χ=1 and interaction scale M_* = 100 GeV.
No excess of events is observed.

TÉCNICO LISBOA LIP

Results

M_χ (GeV)	Yield ($\pm$stat $\pm$syst)	Signal efficiency (%) ($\pm$stat $\pm$syst)	$\sigma^{\text{lim}}_{\text{exp}}$ (fb)	$\sigma^{\text{lim}}_{\text{obs}}$ (fb)
1	$38.3 \pm 0.7 \pm 2.1$	$1.01 \pm 0.02 \pm 0.05$	47^{+21}_{-13}	55
10	$37.8 \pm 0.7 \pm 2.1$	$1.01 \pm 0.02 \pm 0.05$	46^{+21}_{-13}	54
50	$35.1 \pm 0.6 \pm 1.9$	$1.20 \pm 0.02 \pm 0.06$	39^{+18}_{-11}	45
100	$30.1 \pm 0.4 \pm 1.7$	$1.46 \pm 0.02 \pm 0.07$	32^{+14}_{-9}	37
200	$18.0 \pm 0.2 \pm 1.0$	$1.73 \pm 0.02 \pm 0.08$	27^{+12}_{-8}	32
600	$1.26 \pm 0.02 \pm 0.07$	$2.40 \pm 0.03 \pm 0.11$	19^{+9}_{-6}	23
1000	$0.062 \pm 0.001 \pm 0.003$	$2.76 \pm 0.04 \pm 0.13$	17^{+8}_{-5}	20

Confidence levels are obtained through a modified-frequentist CL_s method [47] [48], with both statistical an systematic uncetainties taken into account.

TÉCNICO LISBOA LIP

Results

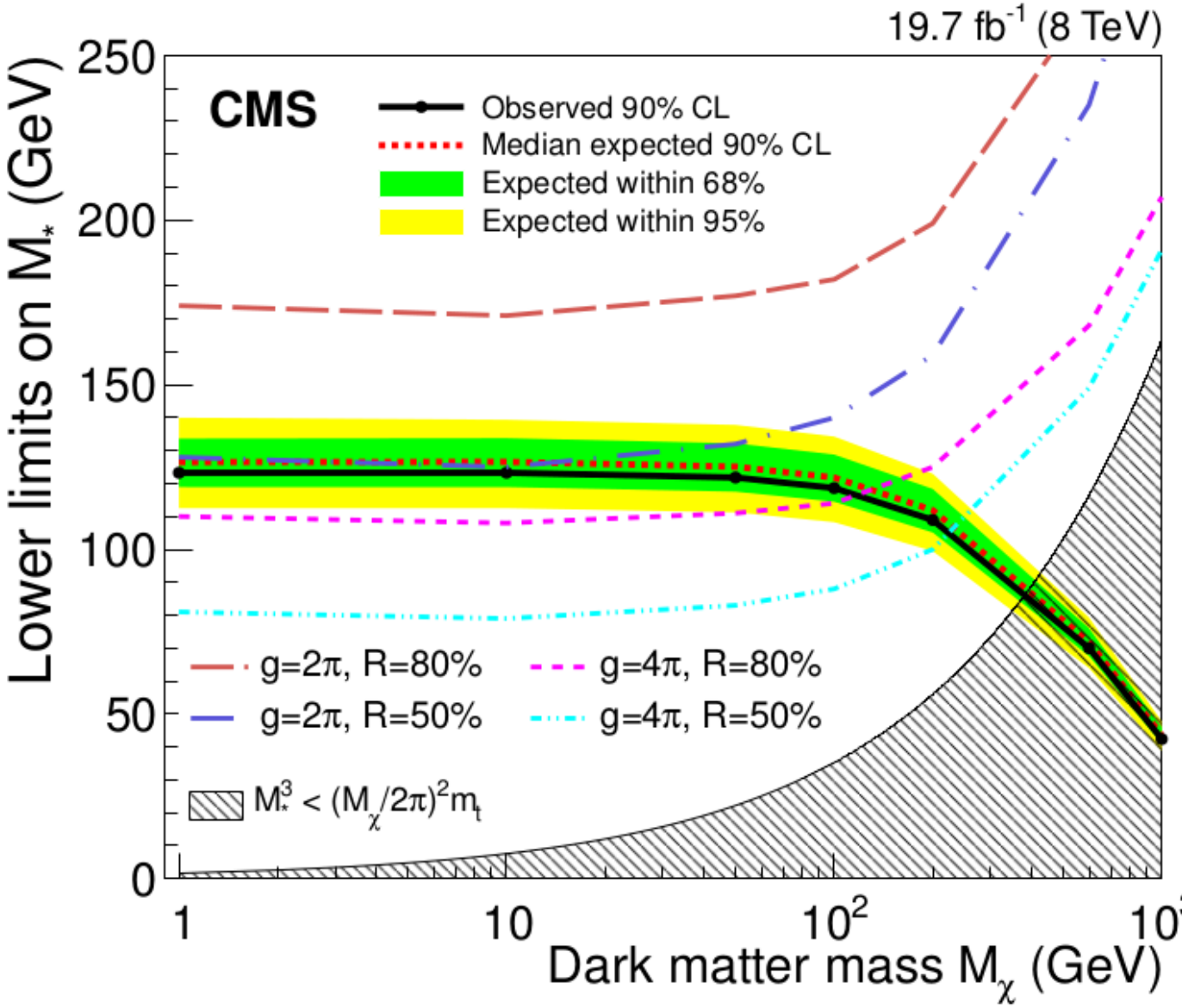
19.7 fb^{-1} (8 TeV)
CMS
Observed 90% CL
Median expected 90% CL
Expected within 68%
Expected within 95%
Lower limits on M$_*$ (GeV)
250
200
150
100
50
0
g=2π, R=80%
g=4π, R=80%
g=2π, R=50%
g=4π, R=50%
M$_*^3$ < (M$_\chi$/2π)^{2}m$_t$
1
10
10^2
10^3
Dark matter mass M$_\chi$ (GeV)

Results

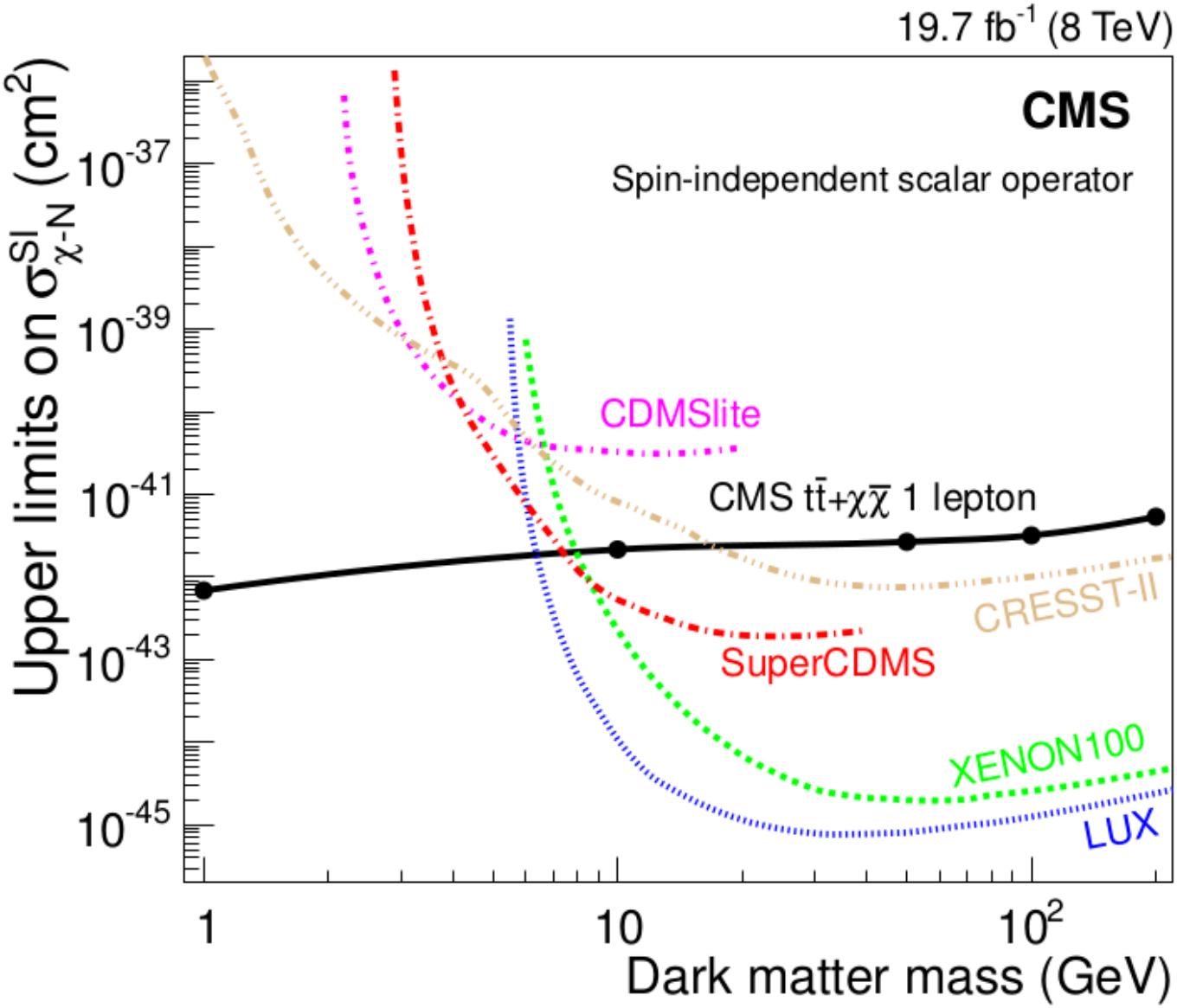
19.7 fb-1 (8 TeV)
CMS
Spin-independent scalar operator
Upper limits on σSIχ-N (cm2)
10-37
10-39
10-41
10-43
10-45
CDMSlite
CMS tt̄+χχ̄ 1 lepton
CRESST-II
SuperCDMS
XENON100
LUX
1
10
10²
Dark matter mass (GeV)

Summary

- A search for the production of dark matter particles in association with top quarks in single-lepton events with the CMS detector at the LHC, using proton-proton collision data.

Summary

- A search for the production of dark matter particles in association with top quarks in single-lepton events with the CMS detector at the LHC, using proton-proton collision data.

- Cross sections larger than 20 to 55 fb are excluded at 90% CL, for a dark matter mass from 1 to 1000 GeV.

Summary

- A search for the production of dark matter particles in association with top quarks in single-lepton events with the CMS detector at the LHC, using proton-proton collision data.
- Cross sections larger than 20 to 55 fb are excluded at 90% CL, for a dark matter mass from 1 to 1000 GeV.
- Lower limits on the interaction scale are set, between dark matter particleas and top quarks in an EFT scalar theory.

Summary

- A search for the production of dark matter particles in association with top quarks in single-lepton events with the CMS detector at the LHC, using proton-proton collision data.
- Cross sections larger than 20 to 55 fb are excluded at 90% CL, for a dark matter mass from 1 to 1000 GeV.
- Lower limits on the interaction scale are set, between dark matter particleas and top quarks in an EFT scalar theory.
- In the case of an s-channel mediator te limits for which the EFT approximation is valid, are interpreted as limits on the dark matter-nucleon scattering cross sections.

TÉCNICO LISBOA LIP

Summary

- A search for the production of dark matter particles in association with top quarks in single-lepton events with the CMS detector at the LHC, using proton-proton collision data.
- Cross sections larger than 20 to 55 fb are excluded at 90% CL, for a dark matter mass from 1 to 1000 GeV.
- Lower limits on the interaction scale are set, between dark matter particleas and top quarks in an EFT scalar theory.
- In the case of an s-channel mediator te limits for which the EFT approximation is valid, are interpreted as limits on the dark matter-nucleon scattering cross sections.
- For masses lower than 6 GeV, more stringent limits are obtained than from direct dark matter searches.

TÉCNICO LISBOA

Thank you for your attention !
Any questions ?